A HIGH-PERFORMANCE ^{14}C ACCELERATOR MASS SPECTROMETRY SYSTEM

M L Roberts[1,2] • J R Burton[1] • K L Elder[1] • B E Longworth[1] • C P McIntyre[1] • K F von Reden[1] • B X Han[3] • B E Rosenheim[4] • W J Jenkins[1] • E Galutschek[1] • A P McNichol[1]

ABSTRACT. A new and unique radiocarbon accelerator mass spectrometry (AMS) facility has been constructed at the Woods Hole Oceanographic Institution. The defining characteristic of the new system is its large-gap optical elements that provide a larger-than-standard beam acceptance. Such a system is ideally suited for high-throughput, high-precision measurements of ^{14}C. Details and performance of the new system are presented.

INTRODUCTION

The National Ocean Sciences Accelerator Mass Spectrometry (NOSAMS) facility at the Woods Hole Oceanographic Institution has recently constructed a new AMS system with large-gap optical elements. The reason for the large-gaps is a gas-accepting microwave-plasma ion source designed in conjunction with Atomic Energy of Canada Limited (Chalk River, Ontario, Canada) and further developed at NOSAMS (Roberts et al. 2007). The prototype of this gas ion source, combined with a magnesium charge-exchange canal, produced reasonable C^- ion currents (on order 60 μA) with low memory, and will allow the analysis of ^{14}C from a continuously flowing stream of sample gas. Unfortunately, the beam from the gas ion source/charge-exchange canal combination has a large emittance and large energy spread. To avoid excessive transmission losses, a custom-built AMS system with large-gap optical elements and energy-stigmatic transport was necessary (Han et al. 2007a).

Although the system was not specifically designed to be used as a "traditional" AMS system, it turns out that, when coupled to a high-output graphite source, the large acceptance of the system has produced a "traditional" AMS system with exceptional performance.

SYSTEM DESCRIPTION

A schematic of the system is shown in Figure 1. The ion-optical elements of the system have gaps that are typically 50% larger than those found in "traditional" compact AMS systems (Synal et al. 2000). Additionally, the low-energy electrostatic analyzer and the low-energy injection magnet form a mass-dispersive, energy-stigmatic analyzing system that compensates almost entirely for the large energy spread in the beam emitted from the gas-accepting ion source. The low-energy electrostatic analyzer was designed to be rotatable and thus allow installation of 2 ion sources on the system. (It should be noted that when the electrostatic analyzer is rotated to the non-gas ion-source direction, it is certainly not an energy-stigmatic system, and is in fact energy dispersive. Nevertheless, this is perfectly suitable for a source that produces a beam with minimal energy spread).

In our case, the second ion source is a modified National Electrostatics Corporation (NEC), MC-SNICS that accepts conventional graphite targets and thus permits traditional AMS measurements. Modifications to the MC-SNICS source have been extensive and include many of the modifications suggested elsewhere (Han et al. 2007b; Southon and Santos 2007) plus a few modifications unique

[1]Woods Hole Oceanographic Institution, Department of Geology and Geophysics, Woods Hole, Massachusetts 02543, USA.
[2]Corresponding author: Email address: mroberts@whoi.edu.
[3]Present address: Research Accelerator Division, SNS, Oak Ridge National Laboratory, Oak Ridge, Tennessee 37831, USA.
[4]Present address: Department of Earth and Environmental Sciences, Tulane University, New Orleans, Louisiana 70118, USA.

Proceedings of the 20th International Radiocarbon Conference, edited by A J T Jull
RADIOCARBON, Vol 52, Nr 2–3, 2010, p 228–235

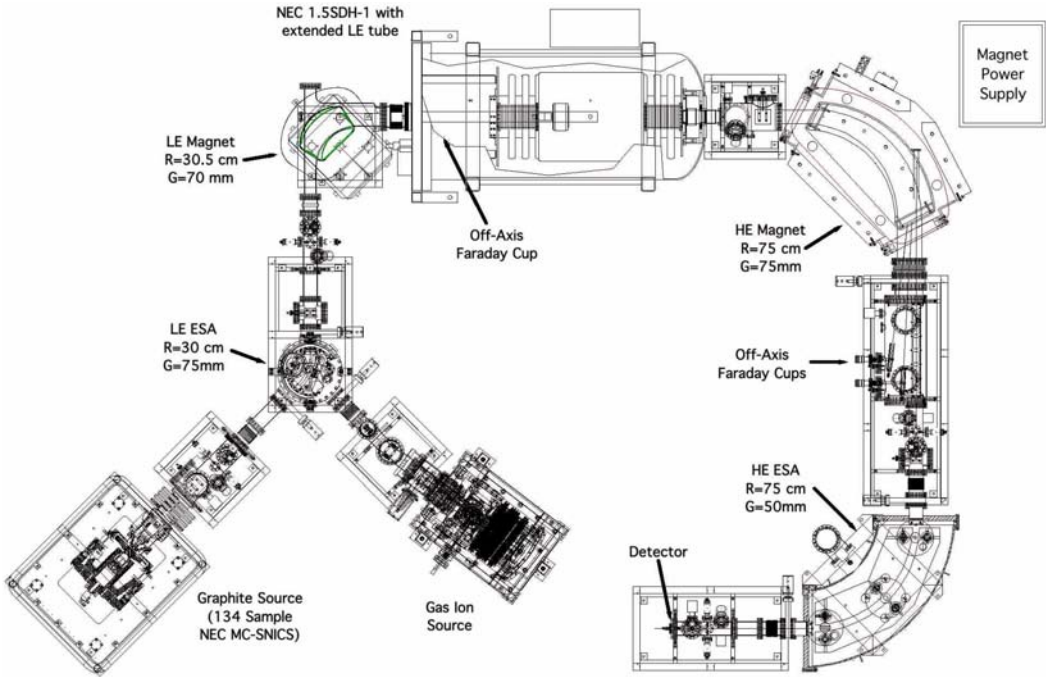

Figure 1 Schematic of the new AMS system. The defining characteristic of the system is the large-gap optical elements.

to our system. These modifications include 1) a cryopump for improved pumping speed (especially for water); 2) a new cesium oven designed to simplify and speed up cesium loading; 3) a vacuum-insulated cesium feed tube that has eliminated tube clogging and greatly reduced the lag time between changes in oven temperature and source response (and as a bonus, eliminated the need for a tube heater power supply); 4) a spherical ionizer and immersion lens for improved cesium focusing; 5) an improved open-geometry extraction/Einzel lens assembly for faster source pump down time and improved source vacuum; and 6) replacement of the NEC acceleration tube with a new high-voltage gap that improves source-to-pump vacuum conductance.

Additionally, we have built a new 134-sample wheel that can be interchangeably used with the standard NEC wheel (Figure 2). The new wheel has a stainless steel outer rim and an aluminum central hub. The stainless steel rim is much easier to clean (and keep clean) than the all aluminum NEC wheel. The inner hub was kept as aluminum to facilitate heat conduction to the central, fluid-cooled, mounting hub. A copper ring is used to improve electrical contact with the spring-loaded high-voltage cathode feedthrough. Sample holders are held in place using side-mounted ball-nosed spring plungers. Sample holders are made of 6061-T6 aluminum and are ~6.3 mm (0.25″) in diameter by 12.7 mm (0.50″) long. The sample hole is "blind" and is 1 mm (0.040″) diameter by 2 mm (0.080″) deep. The sample hole is drilled "dry" just prior to sample pressing to assure no cutting fluid residues are in the hole. Graphite is front-loaded using a hammer and drill blank. The tapered front surface of the sample holder acts as a funnel to assist in the front-loading process. The holders are large enough to be easily labeled, reducing the probability of inadvertently swapping samples. The cost of the sample holders is approximately $0.61 US when bought in quantities of 3000. In using the new wheel, we find that the ion source pumps down much faster after wheel changes, and we see much less out-gassing and cathode sparking as sputtering is initiated. The "old" aluminum wheel, once cesiated, was hard to clean and this probably led to higher retention of water vapor and excessive

electrical discharge under Cs+ sputtering. The stainless steel rim of the new wheel retains a smooth surface and easily wipes clean with a damp Kimwipe.

Figure 2 The 134-sample wheel. The lower insert shows our new front-loading sample holders (right) compared to the NEC sample holders (left).

Control of the entire spectrometer is accomplished using National Instruments PXI hardware and LabVIEW software running on a Windows® XP platform. In our system, hardware modules (e.g. DACs, ADCs, I/Os, etc.) are located in PXI chassis that are peripherally distributed throughout the system. Communication from the PXI chassis to the control computer is done using fiberoptics. Because of the fiberoptic link, we were able to place 1 PXI chassis on the high-voltage platform of the sputter ion-source to control and monitor those associated power supplies. With the LabVIEW software, we have incorporated several aids to beam tuning. For instance, we can automatically scale between the mass 14 and 13 tunes using a single mouse click. Additionally, a "flat-topping" routine allows us to precisely optimize the tune. Other features of the system include full vacuum interlocking, read-back plotting (vacuum, voltage, current, etc.) as a function of time, and closed loop control of magnetic fields. Overall, system loop times are sufficiently fast (>20 Hz) so that there is no noticeable lag between parameter input and beam response.

Data acquisition has been described elsewhere (von Reden et al. 2008) and is accomplished using a combination of National Instruments PXI hardware, NIM and CAMAC modules, and LabVIEW software running on a Windows XP platform.

SYSTEM PARAMETERS

In "traditional" compact AMS systems, the inherent focusing property of the low-energy acceleration tube is used to form a beam waist at the entrance of the stripper canal. The focusing strength is adjusted by ion source energy. In our case, to allow more flexibility in choosing injection energies, we specified the NEC accelerator to have an "extended" low-energy acceleration tube with 2 extra acceleration gaps (20 gaps versus the "standard" 18 gaps). The first 4 gaps of the low-energy acceleration tube have quarter-value resistors (~250 MΩ) while the next 4 gaps have half-value (~500 MΩ) resistors. The effect of the reduced value resistors is a "soft/gentle" acceleration of the incoming ions, and ultimately better beam transmission through the stripper canal. Figure 3 is a plot of transmission efficiency (not to be confused with charge state distribution) as a function of both terminal potential and ion source beam energy. In our case, transmission efficiency is defined as the ratio of the high-energy analyzed $^{12}C^{+}$ current measured on the high-energy off-axis Faraday cup to the low-energy injected $^{12}C^{-}$ current measured at the entrance to the accelerator. With our system, we find that there is little difference in *maximum* transmission efficiency for the various injection energies. We do find that maximum transmission efficiency occurs at a slightly higher terminal potential as the injection energy is raised. In all cases, however, maximum transmission efficiency occurs at stripping energies above 500 keV. This is in contrast to the ^{12}C charge state distribution that has a rather broad maximum around 400 keV (Jacob et al. 2000). In practice, we operate at a terminal potential of 525 kV and an injection energy of between 53 and 63 keV. We prefer the higher injection energies because the resulting reduced beam divergence improves beam transmission through other parts of the low-energy injection system.

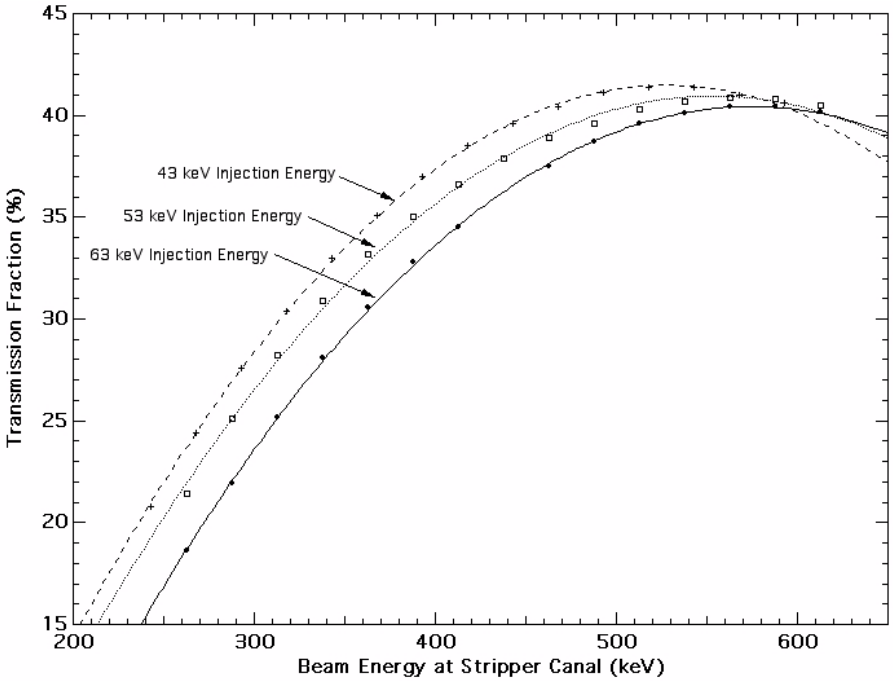

Figure 3 Transmission efficiency as a function of beam energy for various injection energies. The curves are just a guide to the eye. Beam energy at stripper canal is the sum of injection energy and terminal potential.

As shown in Figures 4a,b, transmission efficiency and system background have also been measured as a function of stripper gas pressure. Transmission efficiency is higher at lower canal pressures (Figure 4a). However, incomplete molecular disassociation occurs at lower pressures (Figure 4b). Additionally, at high stripper gas pressures the background rises again, presumably due to the increased multiple scattering events in the acceleration tubes. In our case, we have chosen to run the stripper canal at a pressure near 26 mTorr, yielding a typical system background of $F_m \approx 0.001$ (or >55,000 yr) from Alpha Aesar graphite. Figure 4b also shows results from a sealed-tube graphitization of the VIRI K intercomparison sample. The overall higher background is presumably due to increased hydrides in the prepared sample.

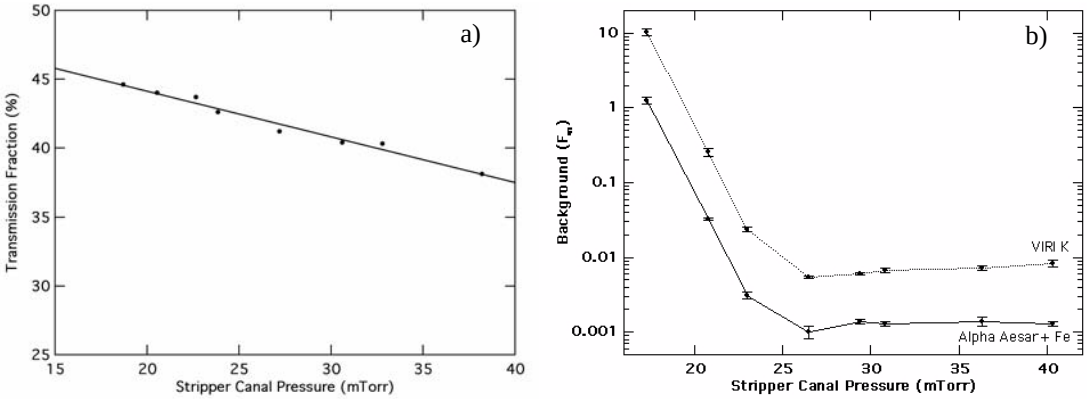

Figures 4 Transmission efficiency and system background as a function of stripper gas pressure. The line in Figure 4a is a best-fit line. In Figure 4b, the upper dashed line and points are from a sealed-tube graphitization of VIRI K. The lower solid line and points are from commercially obtained graphite (Alpha Aesar) mixed with Fe. The lines in Figure 4b just connect the points. All data were taken at a terminal potential of 525 keV at an injection energy of 63 keV.

Typical ion-source parameters are listed in Table 1. From prepared graphite (on 3.5 mg Fe catalyst), we typically see $^{12}C^-$ ion currents of between 125 and 175 μA as measured at the entrance of the accelerator.

Table 1 Typical ion source parameters.

Source high voltage		40 kV	0.3 mA
Extractor voltage		15 kV	0.9 mA
Cathode voltage		8 kV	2.2 mA
Total beam energy		63 kV	
Ionizer	23.5 A	6.9 V	162 W
Cesium oven	0.78 A	32 V	142 °C
$^{12}C^-$current (typical)			125–175 μA
Pump down time after wheel loading			1 hr
Time from wheel loading to data acquisition			2 to 3 hr

Operating the system at high source currents (~175 mA C^-), we observe little (or no) running room when tuning the low-energy magnet. It would appear that the beam is completely filling the stripper canal at the terminal of the accelerator. In our case, the terminal stripper canal is about 450.8 mm (17.75″) long with an entrance diameter of 6.35 mm (0.250″) that has a stepped taper to an exit diameter of 9.53 mm (0.375″). Using ion optic calculations, that included constraints on the beam

divergence based on the low-energy ESA and magnet gaps, and assumed knowledge of the beam dimensions at the stripper canal, we back-calculated a limiting ion source emittance of less than 50 π·mm·mrad at a beam energy of 63 keV. This value is higher than the emittance measurement of 40 π·mm·mrad measured by Southon et al. (2007) at a beam energy of 55 keV. We believe that any further increase in ion source output will only increase the beam emittance, which would require a larger diameter terminal stripper canal.

SYSTEM PERFORMANCE

Performance of the system is illustrated in Figures 5 and 6. Figure 5 shows 80 repeated measurements of a single 430-µg HOxI cathode. Most data points represent the detection of about 30,000 ^{14}C ions (the last 10 data points having between 17,000 and 30,000 counts) with each data point requiring between 100 and 180 seconds to measure. After every fourth data point, normalizing standards, other samples, blanks, secondary standards, etc., were measured. The time between the first and last measurement was about 12 hr. Using the sum of all ^{14}C ions detected in all 80 measurements, a total system efficiency of 8.9% was calculated. Total efficiency is the ratio of measured ^{14}C counts to the number of ^{14}C atoms calculated to be in 430 µg of graphite produced from an oxalic acid standard (HOxI). Correcting for transmission efficiency, bouncer cycling, and system wait times, this total ion source ionization efficiency was calculated to be 24.8%. Similar efficiency results were also obtained from a 390-µg HOxI cathode. Using the NEC style sample holders, the source ionization efficiency was measured to be only 12.5%. We speculate that the dramatic increase in source ionization efficiency is due to our new wheel/sample-holder arrangement. We believe the "blind" hole in our new sample holders (as opposed to the through hole in the NEC holders) allows for "recycling" of sputtered but non-ionized carbon in the sample hole. Our source efficiency measurements are similar to but slightly lower than values reported from the Livermore group (Fallon et al. 2007) from their ion source.

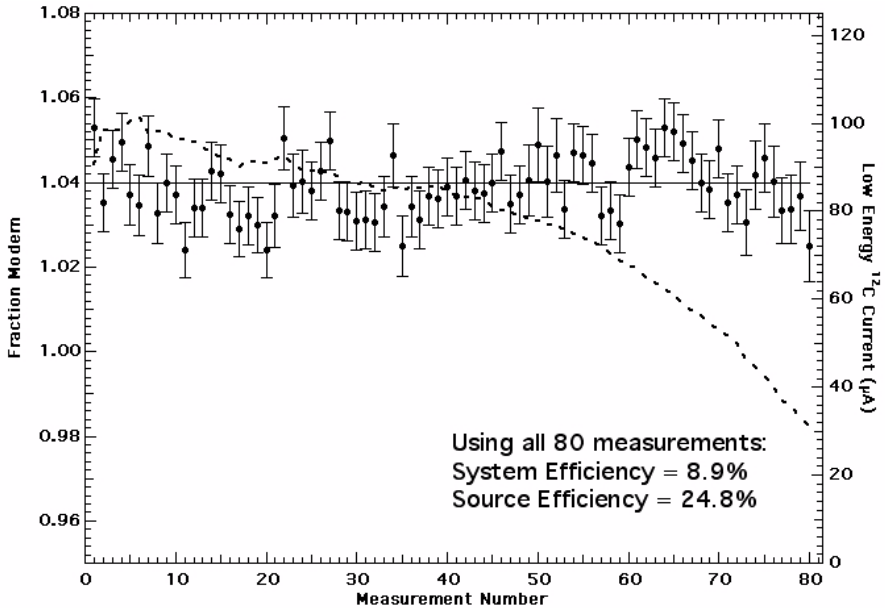

Figure 5 Repeat measurements of a 430-µg HOxI. The uncertainty for each point is a combination of statistical and normalization errors. The average low-energy ^{12}C current (measured on the off-axis Faraday cup) is shown as a dashed line using the right axis. These data demonstrate both the efficiency and stability of the system.

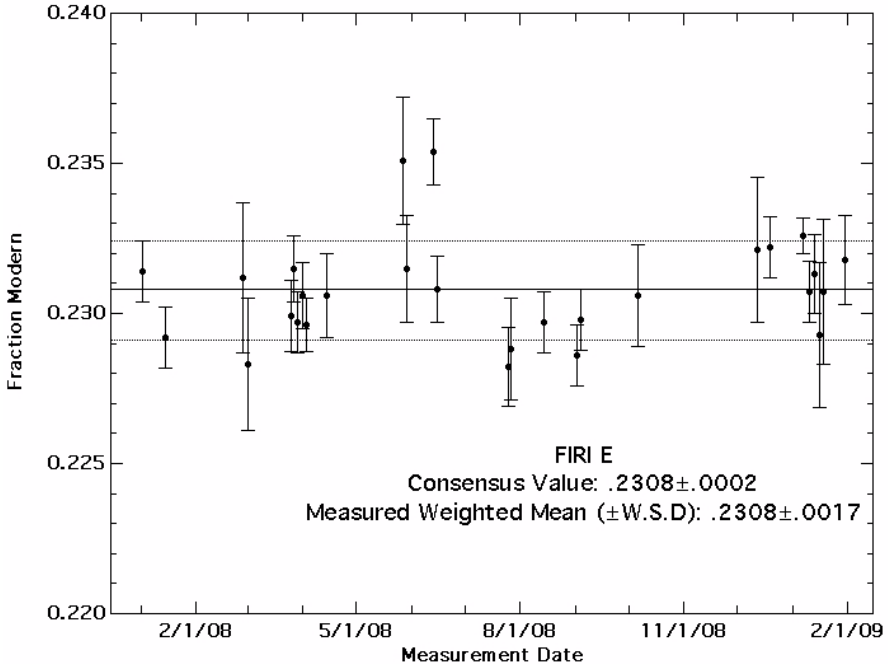

Figure 6 Measurement of the FIRI E sample over the course of about a year. The weighted mean of the 28 individual measurements is identical to the consensus value of Fm = 0.2308. These data demonstrate the repeatability, accuracy, and long-term stability of both the sample preparation methods used and the AMS system.

In addition to system/source efficiency, the data shown in Figure 5 demonstrates the short-term stability of the system. Taking into account normalization error, the individual measurements had errors of between 6.6 and 8.6‰. The standard deviation of the 80 measurements was 7.2‰. Comparing the standard deviation of the individual measurements to the weighed mean, one can infer a systematic (or system) error of <1.2‰ over the 12-hr measurement period. The apparently non-random scatter shown in Figure 5 is partly due to an artifact of data acquisition/reduction in that the measurements were taken in blocks of 4 with each block using the same 6 normalization standards. Cross-correlation (i.e. autocorrelation) of the data set with itself shows no periodic signal buried in the noise except for this sampling artifact.

Figure 6 shows results of approximately a year's worth of repeated measurements of the FIRI E sample (Fourth International Radiocarbon Intercomparison, Sample E, Humic Acid [Scott 2003]). The 28 samples were individually prepared and measured using a sealed-tube graphitization technique and analyzed as an unknown on various wheels. Individual measurement errors ranged from 0.6 to 2.6‰. The measured weighted mean of the various results was essentially the same as the consensus value. These data demonstrate the repeatability, accuracy, and long-term stability of both the sample preparation methods used and the AMS system.

SUMMARY

A new and unique ^{14}C AMS facility has been constructed at the Woods Hole Oceanographic Institution. The defining characteristic of the new system is its large-gap ion-optical elements that provide a larger-than-standard beam acceptance. When coupled to a high-output graphite source, the

large acceptance of the system has produced a "traditional" AMS system with exceptional performance. Precision of 2–3‰ is routinely achieved with a sample to detector efficiency of about 9%. Although the system was not specifically designed to be used as a "traditional" AMS system, the superb performance of the system will make it extremely attractive for various projects that generate samples of small size and/or projects in which high precision is needed.

REFERENCES

Han BX, von Reden KF, Roberts ML, Schneider RJ, Hayes JM, Jenkins WJ. 2007a. Electromagnetic field modeling and ion optics calculations for a continuous-flow AMS system. *Nuclear Instruments and Methods in Physics Research B* 259(1):111–7.

Han BX, Southon JR, Roberts ML, von Reden KF. 2007b. Computer simulation of MC-SNICS for performance improvements. *Nuclear Instruments and Methods in Physics Research B* 261(1–2):588–3.

Jacob SAW, Suter M, Synal H-A. 2000. Ion beam interaction with stripper gas - key for AMS at sub MeV. *Nuclear Instruments and Methods in Physics Research B* 172(1–4):235–41.

Fallon SJ, Guilderson TP, Brown TA. 2007. CAMS/LLNL ion source efficiency revisited. *Nuclear Instruments and Methods in Physics Research B* 259(1): 106–10.

Roberts ML, Schneider RJ, von Reden KF, Wills JSC, Han BX, Hayes JM, Rosenheim BE, Jenkins WJ. 2007. Progress on a gas-accepting ion source for continuous-flow accelerator mass spectrometry. *Nuclear Instruments and Methods in Physics Research B* 259(1):83–7.

Scott EM, editor. 2003. The Third International Radiocarbon Intercomparison (TIRI) and the Fourth International Radiocarbon Intercomparison (FIRI), 1990–2002: Results, Analyses, and Conclusions. *Radiocarbon* 45(2):135–408.

Southon JR, Santos GM. 2007. Life with MC-SNICS. Part II: further ion source development at the Keck Carbon Cycle AMS facility. *Nuclear Instruments and Methods in Physics Research B* 259(1):88–93.

Southon JR, Santos G, Han BX. 2007. Cs feed tests and emittance measurements on a modified MC-SNICS ion source for radiocarbon AMS. *Radiocarbon* 49(2): 301–6.

Synal H-A, Jacob S, Suter M. 2000. The PSI/ETH small radiocarbon dating system. *Nuclear Instruments and Methods in Physics Research B* 172(1–4):1–7.

von Reden KF, Roberts ML, Jenkins WJ, Rosenheim BE, McNichol AP, Schneider RJ. 2008. Software development for continuous-gas-flow AMS. *Nuclear Instruments and Methods in Physics Research B* 266(10): 2233–7.